

## Effect of alkyl derivation on the chemical and antibacterial properties of newly synthesized Cu(II)- diamine complexes

*Ismail Badran<sup>1\*</sup>, Lubna Abdallah<sup>2</sup>, Ruba Mubarakeh<sup>1</sup> Ismail Warad<sup>1\*</sup>*

<sup>1</sup>Department of Chemistry, An-Najah National University P.O. Box 7, Nablus, Palestine

<sup>2</sup>Department of Biology and Biotechnology, An-Najah National University P.O. Box 7, Nablus, Palestine

### Abstract

The effect of alkyl substitution on the chemical and biological properties of Cu(II) diamine compounds was studied by carefully synthesizing two asymmetrical diamine/copper(II) nitrate salt complexes. The unsubstituted complex A and ethyl substituted complex B were synthesized from hydrated copper nitrate salt and the appropriate diamine ligands and identified by elemental analysis, FTIR and UV-Vis spectroscopy. The chemical properties and solvatochromatic behavior of both complexes were studied by UV-Vis. The antibacterial activity of the two complexes was tested against six bacterial isolates which are common pathogens for humans. The results were interpreted under the light of quantum chemical calculations. Time dependent density functional theory was used to interoperate the UV-Vis spectra of both compounds.

\* Corresponding author:

[i.badran@najah.edu](mailto:i.badran@najah.edu)

[warad@najah.edu](mailto:warad@najah.edu)

Received 03 Dec 2018,

Revised 20 Feb 2019,

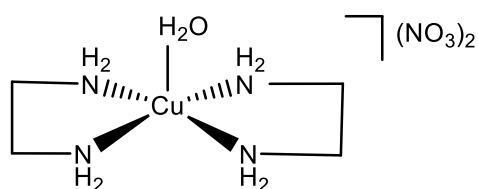
Accepted 24 March 2019

**Keywords:** Cu(II) complexes, diamine ligands, antibacterial, biological activity, theoretical calculations, DFT,

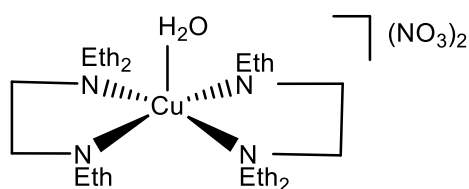
TDDFT, solvatochromism

## 1. Introduction

Success of organometallic complexes in treating modern diseases like cancer is prevailing in medicinal chemistry. Platinum compounds such as cisplatin and carboplatin have led the fight against cancer in recent decades.<sup>1-2</sup> However, platinum based drugs suffer from major drawbacks.<sup>1-3</sup> Many adverse effects such as nephrotoxicity, neurotoxicity, and ototoxicity were reported after using cisplatin. In addition, such drugs are now known for their DNA damaging abilities. Recently, copper based therapeutics (CBTs) have gained attention as good replacements for Pt based drugs.<sup>1-2, 4</sup> Despite the fact that free copper is very toxic to humans, copper (II) complexes were shown to be promising biological treatments.<sup>4-10</sup> Szymański *et. al.* reported that administration of copper ions in the form of a complex can have the ability to deliver Cu ions directly into damaged cells.<sup>6</sup> In their review on Cu(II) complexes, Katwal *et. al.* attributed the biological activity of CBTs on the basis of chelation therapy.<sup>8</sup> The use of broad spectrum and low toxic antibiotics can reduce the efficiency of future antimicrobial therapies.<sup>9</sup> Moreover, the use of restricted antibiotics can cause the failure of antimicrobial therapy and increase the rate of morbidity and mortality.<sup>10</sup> Due to that, several approaches are used to produce antibacterial agents with better activity like copper complexes. Gram-negative bacteria have specialized mechanisms that throughout foreign substances from the cell. These mechanisms prevent the accumulation of antibiotics inside the bacteria and inhibit their actions.<sup>11</sup> In a similar way, Gram-positive bacteria protect themselves with thick cell walls. The peptidoglycan layers of thick walls prevent the passage of hydrophobic compounds.<sup>12</sup> In this study, the two copper complexes, **A** and **B**, were examined against six bacterial isolates which are common pathogens in human diseases. Among them, *Pseudomonas aeruginosa*, which is a widespread Gram-negative bacterium that causes a variety of severe opportunistic infections in immune-compromised individuals, causing significant levels of morbidity and mortality.<sup>13</sup> The other bacterial isolate, *Escherichia coli* is an enteric Gram-negative bacterium. Enteropathogenic strains of *E. coli* produce toxins that cause secretory diarrhoea, commonly called Travellers' diarrhoea.<sup>14</sup> The third studied bacterium is *Klebsiella pneumoniae*. These bacteria are Gram-negative rods that cause bacterial pneumonia and hospital-acquired infections.<sup>15</sup> The last studied Gram-negative bacterium is *Proteus vulgaris*. It has been reported that *P. vulgaris* causes urinary tract infections, wound infections, burn infections, bloodstream infections, and respiratory tract infections.<sup>16</sup> In addition to that, *Staphylococcus aureus* and MRSA were also studied. *S. aureus* is a Gram-positive bacterium which is one of the leading causes of human infections of the skin, soft tissues, bones and joints, abscesses, as well as normal heart valves.<sup>17</sup> Methicillin Resistant *Staphylococcus aureus* (MRSA) is a multiresistant strain that has been documented worldwide showing rising resistance to different classes of antimicrobials.<sup>18</sup> Recently, we synthesized a series of Cu(II) diamine and oxime complexes and examined their chemical and electronic properties.<sup>11-13</sup> The newly synthesized complexes were shown to be thermally stable, and exhibits interesting chemical properties such as solvatochromic shifts. Solvatochromism is the ability of a chemical substance to change color due to interactions with polar solvents. Although the exact mechanism behind this phenomena is still unknown,<sup>14</sup> solvatochromism has many applications in the field of chemical sensors, molecular switches, and to describe solvent parameters. For instance, Zhang *et. al.*, have engineered a novel methyl ketone bridged molecule by utilizing its basochromism behavior.<sup>15</sup> While recently, the phenomena was used to synthesize an efficient fluorescence emitter.<sup>16</sup> In this work, we synthesized the Cu(II) diamine complex (complex A), in order to investigate its chemical and biological activity. Also, we synthesized a modified derivative of the compound, complex B, by adding ethyl groups as shown below. This allowed us to understand the role of alkylation of Cu(II) complexes on their antibacterial activity, as well as their solvatochromic shifts.



Complex A



Complex B

In addition to the biological study, and based on our previous reports on similar Cu(II) complexes, the solvatochromism behavior of the two synthesized complexes was investigated by recording the UV-Vis spectra in water and other common organic solvents.

## 1. Materials and Methods

### 2.1 Chemicals

All the reagents, diamines and copper(II) salt were purchased from Sigma–Aldrich. The FT-IR was performed in range 400–4000  $\text{cm}^{-1}$  using Perkin–Elmer 621 instrument. CHN-Microanalysis was carried out on an EL Elementar-Varrio analyzer. Pharmacia LKB-Biochrom 4060 served to measure UV-Vis absorption spectra.

### 2.2 Synthetic procedure

More details on the synthesis procedure are found elsewhere.<sup>11, 13</sup> Under ultrasonic mode of vibration, 1 mmol of  $\text{Cu}(\text{NO}_2)_2 \cdot 2\text{H}_2\text{O}$  was dissolved in 10 mL of ethanol. Under continuous stirring, 1 mmol of diamine was dissolved in 5 mL of water and was added drop-wise to the copper(II) solution. The color of the mixture was changed from brown to blue within 10 min. The solvents were evaporated under vacuum; the solid product powder was washed with diethyl ether then lifted to room temperature. Blue color complexes were collected in a good yield. Complexes **A** and **B** were identified by their melting points, FTIR spectra, and HCN elemental analysis as described below. Because detailed XRD analysis was performed on similar complexes in our previous work,<sup>13</sup> no further XRD analysis was needed.

#### 2.2.1 Complex A

88% yield, m.p. = 198 °C, MS  $m/z$  201.08 (201.3 theoretical) of  $[\text{M}-(\text{N}_2)_2]-2\text{NO}_3$ , CHN-analysis Cald: C, 14.75; H, 5.57; N, 25.80, for  $\text{C}_4\text{H}_{18}\text{CuN}_6\text{O}_7$  Found C, 14.55; H, 5.43; N, 25.65%, IR (KBr,  $\text{cm}^{-1}$ ): 3350 ( $\nu_{\text{H}_2\text{O}}$ ), 3255 and 3235 ( $\nu_{\text{H-N}}$ ), 2945 ( $\nu_{\text{C-H}}$ ), 1410 ( $\nu_{\text{NO}_3}$ ), 1145 ( $\nu_{\text{N-C}}$ ), 515 ( $\nu_{\text{Cu-N}}$ ). UV-vis in water:  $\lambda_{\text{max}}$  260 nm ( $2.6 \times 10^4 \text{ M}^{-1}\text{L}^{-1}$ ) and 565 nm ( $1.5 \times 10^2 \text{ M}^{-1}\text{L}^{-1}$ ).

#### 2.2.2 Complex B

78% yield, m.p. = 208 °C, MS  $m/z$  367.2 (367.7 theoretical) of  $[\text{M}-(\text{N}_2)_2]-2\text{NO}_3$ , CHN-analysis Cald: C, 39.05; H, 8.19; N, 17.08, for  $\text{C}_{16}\text{H}_{40}\text{CuN}_6\text{O}_7$  Found C, 39.01; H, 8.08; N, 17.02%, IR (KBr,  $\text{cm}^{-1}$ ): 3340 ( $\nu_{\text{H}_2\text{O}}$ ), 3230 and 3220 ( $\nu_{\text{H-N}}$ ), 2920 ( $\nu_{\text{C-H}}$ ), 1430 ( $\nu_{\text{NO}_3}$ ), 1140 ( $\nu_{\text{N-C}}$ ), 517 ( $\nu_{\text{Cu-N}}$ ). UV-vis in water:  $\lambda_{\text{max}}$  265 nm ( $2.7 \times 10^4 \text{ M}^{-1}\text{L}^{-1}$ ) and 560 nm ( $1.6 \times 10^2 \text{ M}^{-1}\text{L}^{-1}$ ).

### 2.3 Theoretical calculations

The theoretical calculations in this work are described in previous publications.<sup>13, 17-18</sup> Briefly, the copper complexes, **A** and **B**, were optimized to their equilibrium geometries using Gaussian 09.<sup>19</sup> Frequency calculations were requested

beyond successful optimization in order to characterize the structures' minima. Therefore, no imaginary frequencies were observed. In our previous work on similar complexes,<sup>13</sup> it was shown that the hybrid density functional theory (DFT) functional, BHandH<sup>20</sup>, provided excellent results for optimizing Cu(II) complexes. Therefore, this functional along with the 6-31+G(2d,p) basis set was implemented across this work. In order to obtain the theoretical UV-Vis spectra of the Cu(II) complexes, time-dependent density functional theory (TDDFT)<sup>21-22</sup> calculations were also performed under the same level of theory. TDDFT jobs were carried out on optimized geometries of complexes **A** and **B** by probing the first twenty excited states with regular population. Optimized structures and UV spectra were viewed using Gaussview.<sup>23</sup>

#### 2.4 UV-Vis Analysis

For the UV-Vis analysis of the prepared complexes, a stock solution of each complex was prepared by dissolving 0.01 g of the complex in 10.0 ml of solvent. Different concentrations were then prepared by successive dilution. The samples were then examined using 3 ml quartz cells in a UV-Vis spectrophotometer (Shimadzu, UV-1800). In order to investigate the solvatochromism of the prepared complexes, four solvents were examined; water, acetone, dimethyl sulfoxide (DMSO), and methanol. Analytical grade solvents were purchased from Aldrich. Spectra were recorded and averaged over three runs.

#### 2.5 Preparation of bacterial isolates

Antibacterial sensitivity tests for the two studied Cu-complexes were performed against three reference bacterial isolates which are *Staphylococcus aureus* (ATCC25923), *Escherichia coli* (ATCC 25922) and *Pseudomonas aeruginosa* (ATCC 27853). All obtained from the American Type Culture Collection (ATCC). In addition to three clinical isolates which are Methicillin resistant *Staphylococcus aureus* (MRSA), *Klebsiella pneumoniae* and *Proteus vulgaris* that were obtained from a local hospital (Rafidia Hospital, Nablus, Palestine), and identified by the Biology and Biotechnology Laboratory at An-Najah National University, Palestine. The two synthesized Cu-complexes were dissolved to the desired concentrations using distilled water. Then each prepared solution was sterilized by microfiltration.

#### 2.6 Antibacterial activity of copper complexes

Disk diffusion method was performed to evaluate the antibacterial activity of the two Cu-complexes.<sup>24</sup> All bacterial isolates were grown overnight on nutrient agar plates, then their turbidities were adjusted to 0.5 McFarland (1.5×10<sup>8</sup> CFU/ml). Mueller Hinton agar plates were inoculated by streaking their surfaces with the adjusted bacterial isolates. This procedure is repeated by streaking two more times, rotating the plate approximately 60° each time to ensure an even distribution of the inoculum. As a final step, the rim of the agar was also swabbed. After that, 2000 µg/ml of each complex under study was loaded to 6 mm disk and then the prepared disks were added to the surfaces of inoculated agar plates. All plates were incubated at 37°C for 18 h. After incubation all plates were examined for bacterial growth inhibition by measuring the inhibition zone diameter (IZD) to the nearest mm. The test was performed in triplicates. Antibiotic Gentamicin (G) was used as positive control.

## 2. Results and Discussion

### 3.1 Solvatochromism in copper complexes, A and B

**Figure 1** depicts the optimized structures of complexes **A** and **B** cations as obtained using our DFT calculations at BHANDH/6-31+G(2d,p) level of theory. The structure of complex **B** depicts the “trans, trans” isomer where ethyl

groups are pointing at opposite directions. Other cis conformers were optimized and were found to be less stable in energy. In addition, the main structural parameters of the two complexes cations are tabulated in **Table 1**. The dihedral angle around the copper center is almost flat ( $7.2^\circ$ ) in complex **A**. The four Cu-N bond lengths are almost equal to 2.0 Å, indicating a high symmetrical square pyramidal structure of complex **A**. With the ethyl groups' substitution in complex **B**, this symmetry is highly distorted. This is illustrated by the high deviation from planarity with a dihedral angle of  $35.5^\circ$ . In addition, Jahn Teller distortion was observed upon moving from complex **A** to **B**. The Cu-H<sub>2</sub>O bond length in complex **B** (3.279 Å) is well elongated than that of complex **A** (2.275 Å). Beyond obvious steric hindrance factors, this elongation might be due to enhanced  $\pi$  backbonding from the ethyl-substituted diamine ligands to the copper ion. It is known that alkyl groups are sigma-donors, that strengthen the Cu-N bonds, which leads to more Cu-H<sub>2</sub>O weakening,<sup>25</sup>

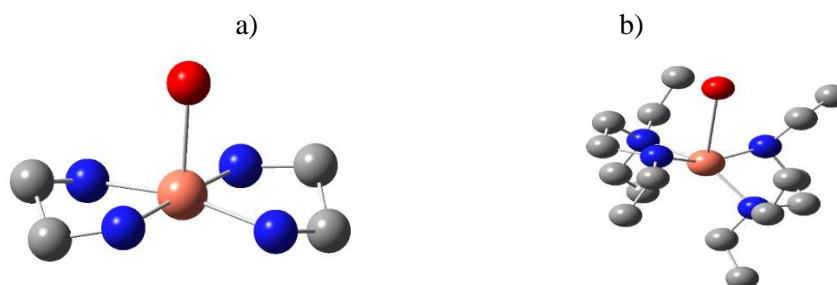


**Figure 1.** Optimized structures and for a) complex **A**, and b) complex **B**, obtained at BHANDH/6-31+G(2d,p) level of theory. C atom, grey; N atom, blue; O atom: Red, H atoms are not shown.

**Table 1.** Structural parameters for complexes **A** and **B** obtained at obtained at BHANDH/6-31+G(2d,p) level of theory

Parameter	Complex A	Complex B
Cu-N1	2.0155 Å	2.0381 Å
Cu-N2	2.0071 Å	1.9826 Å
Cu-N3	2.0049 Å	2.0374 Å
Cu-N4	2.0174 Å	2.0491 Å
Cu-O	2.2746 Å	3.2791 Å
N1-N2-N3-N4	$7.2^\circ$	$35.5^\circ$

Recently, we reported that Cu(II) diamine complexes exhibits strong solvatochromic shifts, due to d-d electron transition in the copper ion center as a result of solute-solvent interactions.<sup>11, 13</sup> The solvatochromism behavior of complexes **A** and **B** was studied by comparing their UV-Vis spectra in different solvents. **Figure 2(a)** shows the absorption spectra of complex **A** in different solvents as obtained from the UV-Vis spectrophotometer. The theoretical spectrum of the same complex is also shown in **Figure 2(b)**. The spectrum was obtained by employing TDDFT calculations on the optimized structure as explained in the theoretical methods section. The good agreement between the two spectra indicates the validity of the calculation method used in this work, and the success of the BHandH functional in predicting accurate spectra for copper(II) complexes. Similar plots for the experimental and theoretical of UV-Vis spectra are shown in **Figure 3**. By comparing the theoretical UV-Vis spectra of complexes **A** and **B**, it is clear that ethyl substitution on the diamine group has red shifted the spectrum. In other words, the theoretical  $\lambda_{\max}$  for complex **A** is 550 nm, while it is 650 nm for complex **B**. this is evident by the visible blue and green colors of complexes **A** and **B**, respectively. Interestingly, Ethyl substitution does not only change the complex color, but also lead to strong bathochromic shift (shift to higher wavelengths) when different solvents were used. When comparing the

UV-Vis spectra of complex **A** (Figure 2,a) to that for complex **B** (Figure 3,a), solvatochromism is strong stronger in complex **B**. the relationship between solvent polarity and solvatochromism behavior in Cu(II) complexes was discussed in our recent works.<sup>11, 13</sup>

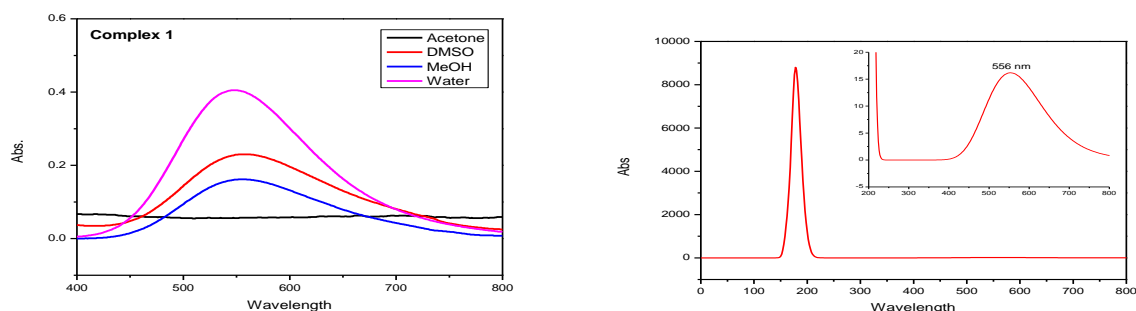


**Figure 2.** a) Experimental absorption spectra of complex **A** in selected solvents, b) Theoretical spectrum obtained by TDDFT theoretical calculations at uBHandH/6-31 p g(2d,p) level of theory. (Inset, zoom in the region of 200-800 nm)

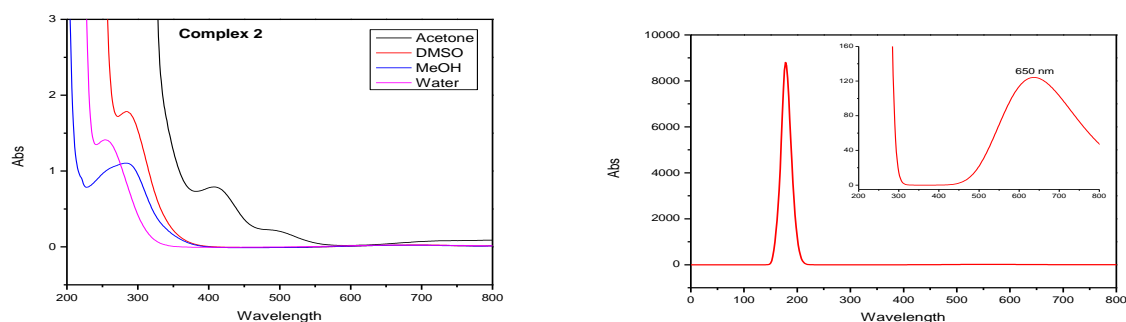


**Figure 3.** a) Experimental absorption spectra of complex **B** in selected solvents, b) Theoretical spectrum obtained by TDDFT theoretical calculations at uBHandH/6-31 p g(2d,p) level of theory. (Inset, zoom in the region of 200-800 nm)

**Table 2.** The first ten excited states of complexes **A** and **B** obtained using TDDFT at uBHandH/6-31+g(2d,p) level of theory.

Complex A					Complex B			
Excited State	excitation energy (eV)	wavelength (nm)	oscillator strength (f)	S <sup>2</sup>	excitation energy (eV)	wavelength (nm)	oscillator strength (f)	S <sup>2</sup>
1	1.86	667.8	0.0000	0.751	1.91	649.1	0.0016	0.752
2	2.20	563.8	0.0000	0.751	1.97	629.5	0.0009	0.752
3	2.23	556.9	0.0002	0.751	2.00	619.5	0.0005	0.752
4	2.25	550.2	0.0002	0.751	2.05	604.5	0.0001	0.752
5	6.55	189.2	0.0560	0.789	5.08	243.9	0.1030	0.799
6	6.73	184.3	0.0001	1.237	5.45	227.6	0.0861	0.791
7	6.98	177.7	0.0018	0.785	5.49	225.8	0.0026	0.783
8	6.98	177.6	0.1924	0.823	6.38	194.3	0.0195	0.808
9	7.43	166.9	0.0000	1.147	7.18	172.6	0.0004	0.796
10	7.56	163.9	0.0377	1.376	7.23	171.6	0.0020	0.971

**Table 2** lists the first ten excited states for complexes **A** and **B** as obtained from our TDDFT calculations. The table lists the excitation energies in units of eV, the wavelength in nm, the oscillator strength (f), as well as the  $S^2$  values. The square multiplicity value ( $S^2$ ) is equal to  $S(S+1)$ . Most  $S^2$  values are close to 0.75 in agreement with doublet multiplicity of the Cu(II) cation complexes **A** and **B**. By investigating the UV-Vis spectra in **figures 2** and **3**, and the results in **Table 2**, one could notice that complex **A** has the first two excited states with an oscillator strength of zero, making them forbidden for electronic transitions. This is followed by a doubly degenerate excited states, 3 and 4, with an excitation wavelength of *ca.* 550 nm which is close to the experimental value of  $\lambda_{\text{max}}$ . Similarly, Complex **B** has an experimental  $\lambda_{\text{max}}$  of *ca.* 650 nm. This is close to the first excited state (649.1 nm) that has an oscillator strength of 0.0016. It is interesting to see how ethyl groups' substitution of complex **A** to convert to complex **B** has caused the first excited states to be symmetry allowed.

### 3.2 Antibacterial activity of copper complexes

Drugs based on metal complexes represent one of the antimicrobial groups that are used for the control of different infectious diseases.<sup>26</sup> Several studies showed that metal complexes with copper ions penetrate more easily through the bacterial cell walls, due to the proteic denaturation of the sulphhydryl groups.<sup>27</sup> This study was conducted to evaluate the antibacterial efficacy of two complexes **A** and **B** against four Gram-negative and two Gram-positive bacterial isolates. Agar disk diffusion results (**Figure 4** and **Figure 5**) indicated that both complexes were able to act against all studied bacteria. This elucidate the broad spectrum antibacterial behavior of the two complexes which could be mediated by either targeting the essential steps in bacterial growth or causing metabolic toxicity.<sup>28</sup> In addition to that the obtained results showed that the inhibition behavior of **B** complex against all examined bacterial isolates was more than 10 mm IZD. Therefore, **B** complex was more effective antibacterial agent than **A** complex in the current study. The possible explanation for that is lipophilicity or hydrophobicity of the Cu-complexes. By consideration of the structure of **B** complex; it exhibited more lipophilic properties than **A** complex (**Figure 4**). In general drug disposition depend on its ability or inability to cross membranes and this correlate with drug lipophilicity. Moreover, many of the proteins involved in drug disposition have hydrophobic binding sites, this also explain the importance of drug lipophilicity. The high permeability of complex **B** may cause DNA cleavage at high concentrations. This could produce a better antimicrobial effect against *S. aureus* and MRSA.<sup>29</sup> In addition to lipophilic effect, copper complexes have plasticity as they are capable of assuming different shapes with different coordination numbers and thus adopt to substrate.<sup>30</sup> Therefore, it was easy to adopt certain geometry and thus avoid possible steric hindrance during their physiological action.<sup>31</sup> Furthermore, the obtained results clearly showed that *P. aeruginosa* was the most sensitive isolate to both **A** and **B** complexes (13 and 14 mm IZD respectively) when compared to the broad spectrum antibiotic Gentamicin (17 mm IZD). The observed variation in the activity of both copper complexes against various types of the studied bacteria may be due to the differences in bacterial cell wall and cell membrane structures.<sup>7</sup> Also the differences in ribosome's of bacterial cells lead to varied activities of the examined complexes.<sup>32</sup> The low and moderate activity of both complexes should be further investigated by analyzing their quorum sensing behavior. The diamine copper complexes synthesized by *Stanojevic et al* act as quorum sensing inhibitors.<sup>31</sup> The inhibition effect attenuates virulence without affecting bacterial growth. As a result, these complexes offering a lower risk for resistance development.

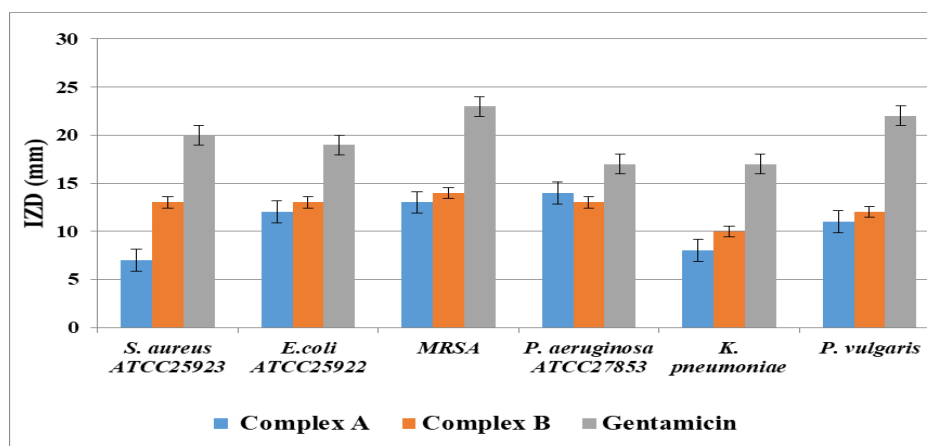


**Figure 4.** Antibacterial activity of Cu-complexes (2000  $\mu\text{g}/\text{disk}$ ) using the agar disk diffusion method; (IZD) inhibition zone diameter.

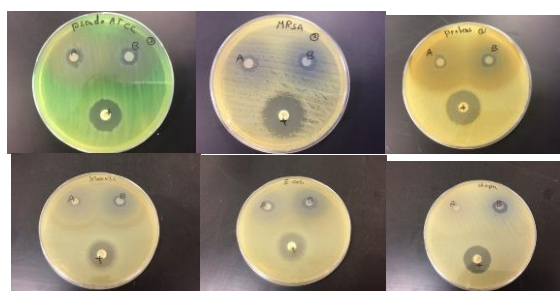


**Figure 5.** Antibacterial activity of Cu-complexes (2000  $\mu\text{g}/\text{disk}$ ) using agar disk diffusion method. A ( ), B ( ), and + (antibiotic Gentamicin).

## CONCLUSION

In this work, two different Cu(II)/diamine compounds were synthesized in order to investigate the effect of alkyl derivation on the chemical and biological behavior of copper(II) complexes. Complex **A**, bearing no alkyl derivations, and complex **B**, containing ethyl substitutions in trans positions, were tested against four known Gram-negative and two known Gram-positive bacterial isolates. Both complexes showed high activity in attacking the bacteria, with complex **B** being the more active. Complex **B** relative activity was attributed to the ethyl groups attached to the diamine ligand. Using *ab-initio* methods, the geometry and structural parameters of both complexes were presented. The mixed density functional BHANDH showed high success in optimizing and predicating the UV-Vis spectra of both complexes, in accordance to previous studies by our group. Strong Jahn Teller distortion was observed in complex **B** relative to **A**. The Cu-H<sub>2</sub>O elongation was attributed to  $\pi$  backbonding from the ethyl-substituted diamine ligands to the Cu atom. In addition, strong solvatochromic shifts were observed in complex **B**, due to the same reasoning. TDDFT calculations using the same BHANDH functional showed that ethyl substitution in complex **B** has allowed the first excited states to be symmetry allowed, which causes the solvatochromic shift to take place.



## REFERENCES

1. Wehbe, M.; Leung, A. W. Y.; Abrams, M. J.; Orvig, C.; Bally, M. B., *Dalton Transactions* **2017**, 46 (33), 10758-10773.
2. Santini, C.; Pellei, M.; Gandin, V.; Porchia, M.; Tisato, F.; Marzano, C., *Chemical reviews* **2013**, 114 (1), 815-862.
3. Holmes, D., *Nature* **2015**, 527 (7579), S218-S219.
4. Glišić, B. Đ.; Aleksic, I.; Comba, P.; Wadepohl, H.; Ilic-Tomic, T.; Nikodinovic-Runic, J.; Djuran, M. I., *RSC Advances* **2016**, 6 (89), 86695-86709.
5. Rocha, D. P.; Pinto, G. F.; Ruggiero, R.; Oliveira, C.; Guerra, W.; Fontes, A. P. S.; Tavares, T. T.; Marzano, I. M.; Pereira-Maia, E. C., *Quím. Nova* **2011**, 34, 111-118.
6. Szymański, P.; Frączek, T.; Markowicz, M.; Mikiciuk-Olasik, E., *BioMetals* **2012**, 25 (6), 1089-1112.
7. Joseph, J.; Nagashri, K.; Rani, G. A. B., *Journal of Saudi Chemical Society* **2013**, 17 (3), 285-294.
8. Katwal, R.; Kaur, H.; Kapur, B. K., *Sci Rev Chem Commun* **2013**, 3 (1), 1-15.
9. Mohamed, G. G.; Zayed, E. M.; Hindy, A. M. M., *Molecular and Biomolecular Spectroscopy* **2015**, 145, 76-84.
10. Ghosh, M.; Fleck, M.; Mahanti, B.; Ghosh, A.; Pilet, G.; Bandyopadhyay, D., *Journal of Coordination Chemistry* **2012**, 65 (22), 3884-3894.
11. Warad, I.; Awwadi, F. F.; Abd Al-Ghani, B.; Sawafta, A.; Shivalingegowda, N.; Lokanath, N. K.; Mubarak, M. S.; Ben Hadda, T.; Zarrouk, A.; Al-Rimawi, F.; Odeh, A. B.; Barghouthi, S. A., *Ultrasonics Sonochemistry* **2018**, 48, 1-10.
12. Saleemh, F. A.; Musameh, S.; Sawafta, A.; Brandao, P.; Tavares, C. J.; Ferdov, S.; Barakat, A.; Ali, A. A.; Al-Noaimi, M.; Warad, I., *Arabian Journal of Chemistry* **2017**, 10 (6), 845-854.
13. Warad, I.; Musameh, S.; Badran, I.; Nassar, N. N.; Brandao, P.; Tavares, C. J.; Barakat, A., *Journal of Molecular Structure* **2017**, 1148, 328-338.
14. Marini, A.; Muñoz-Losa, A.; Biancardi, A.; Mennucci, B., *The Journal of Physical Chemistry B* **2010**, 114 (51), 17128-17135.
15. Zhang, Y.-M.; Wang, X.; Zhang, W.; Li, W.; Fang, X.; Yang, B.; Li, M.; Zhang, S. X.-A., *Light: Science & Applications* **2015**, 4, e249.
16. Etherington, M. K.; Franchello, F.; Gibson, J.; Northey, T.; Santos, J.; Ward, J. S.; Higginbotham, H. F.; Data, P.; Kurowska, A.; Dos Santos, P. L.; Graves, D. R.; Batsanov, A. S.; Dias, F. B.; Bryce, M. R.; Penfold, T. J.; Monkman, A. P., *Nature Communications* **2017**, 8, 14987.
17. Badran, I.; Rauk, A.; Shi, Y. J., *Journal of Physical Chemistry A* **2012**, 116 (48), 11806-11816.
18. Manasrah, A. D.; El-Qanni, A.; Badran, I.; Carbognani Ortega, L.; Perez-Zurita, M. J.; Nassar, N. N., *Reaction Chemistry & Engineering* **2017**, 2 (5), 703-719.
19. Frisch, M.; Trucks, G.; Schlegel, H. B.; Scuseria, G.; Robb, M.; Cheeseman, J.; Scalmani, G.; Barone, V.; Mennucci, B.; Petersson, G., *Inc., Wallingford, CT* **2009**, 200.
20. Becke, A. D., *Journal of Chemical Physics* **1993**, 98 (2), 1372-1377.
21. Casida, M. E.; Jamorski, C.; Casida, K. C.; Salahub, D. R., *Journal of Chemical Physics* **1998**, 108 (11), 4439-4449.
22. Stratmann, R. E.; Scuseria, G. E.; Frisch, M. J., *Journal of Chemical Physics* **1998**, 109 (19), 8218-8224.
23. Dennington, R.; Keith, T.; Millam, J., GaussView, version 5. **2009**.
24. Wayne, P., *Performance standards for antimicrobial disc susceptibility testing* **2002**, 12, 01-53.
25. Miessler, G. L.; Tarr, D. A., *Inorganic chemistry*. 4th ed.; Pearson Prentice Hall: Upper Saddle River, NJ, 2011; p xiv, 754 p.

26. Scozzafava, A.; Menabuoni, L.; Mincione, F.; Mincione, G.; Supuran, C. T., *Bioorganic & medicinal chemistry letters* **2001**, *11* (4), 575-582.
27. Goulart, D. S., Detecção de resíduos de soluções sanitizantes empregadas em pedilúvio para bovinos no leite e solo. **2011**.
28. Srinivasan, D.; Nathan, S.; Suresh, T.; Perumalsamy, P. L., *Journal of ethnopharmacology* **2001**, *74* (3), 217-220.
29. Rajalakshmi, S.; Fathima, A.; Rao, J. R.; Nair, B. U., *RSC Advances* **2014**, *4* (60), 32004-32012.
30. Bacci, M., *New journal of chemistry* **1993**, *17* (1-2), 67-70.
31. Stanojević, I. M.; Aleksić, I.; Drašković, N. S.; Glišić, B. D.; Vojnović, S.; Nikodinović-Runić, J., *J. Serb. Chem. Soc.* **2017**, *82* (12), 1357-1367.
32. Patil, S. A.; Naik, V. H.; Kulkarni, A. D.; Badami, P. S., *Molecular and Biomolecular Spectroscopy* **2010**, *75* (1), 347-354.